Supporting Information

High Performing Ternary Solar Cells through Förster Resonance Energy Transfer between Non-fullerene Acceptors

Lei Yang[†,§], Wenxing Gu[†,‡,§], Ling Hong[†], Yang Mi[‖], Feng Liu[⊥], Ming Liu[†], Yufei Yang[†], Bigyan Sharma[†], Xinfeng Liu[‖], and Hui Huang*[†]

[†]College of Materials Science and Opto-electronic Technology & CAS Key Laboratory of Vacuum Physics, University of Chinese Academy of Sciences, Beijing, 101408, P. R. China.

[‡]School of Electronic, Electrical and Communication Engineering, University of Chinese Academy of Sciences, Beijing, 101408, P. R. China.

[⊥]Department of Physics and Astronomy, Shanghai Jiaotong University, Shanghai 200240, China.

[‖]Division of Nanophotonics, CAS Key Laboratory of Standardization and Measurement for Nanotechnology, CAS Center for Excellence in Nanoscience, National Center for Nanoscience and Technology, Beijing 100190, P. R. China.

Corresponding Author: huihuang@ucas.ac.cn

Characterization

^{1}H NMR and ^{13}C NMR spectra were measured on a Bruker AVANCE 400 MHz NMR spectrometer. Mass spectra were estimated on a Bruker Autoflex III Mass Spectrometer. Elemental analysis was measured on a FLASH EA 1112 elemental analyzer. The electrochemical cyclic voltammetry (CV) was measured in a 0.1 mol/L tetrabutylammonium hexafluorophosphate (Bu_4NPF_6) chloroform solution as the supporting electrolyte with a scan speed at 0.05 V/s. A ferrocene/ferrocenium redox couple was used as an external standard. A Pt

wire, glassy carbon discs, and Ag/AgCl were used as the counter, working electrode, and reference electrodes, respectively. UV-vis absorption spectra were carried out using a Gary 60 UV-vis Spectrophotometer. All the film samples were spin casted on glass substrates. The morphology of blend films was observed by using a Scanning Probe Microscope-Dimension 3100 in tapping mode. The transmission electron microscopy (TEM) characterization was measured on a HITACHI HT 7700. All film samples were spin casted on ITO/ZnO substrates. GIXD characterization was measured on beamline 7.3.3 Lawrence Berkeley National Lab and samples were prepared on Si substrates. RSoXS was carried out at beamline 11.0.1.2 Lawrence Berkeley National Lab and samples were prepared on Si/PEDOT:PSS substrates. Fluorescence lifetimes were determined with steady state spectrometer FLS980. Transient Absorption spectroscopy has been performed by HELIOS (Ultrafast Systems).

Fabrication and characterization of polymer solar cells

Inverted solar cells consisted of a stack glass/ITO/ZnO/ active layer/ MoO_3/Ag. The pre-patterned ITO was cleaned by ultrasonic agitation in detergent, deionized water, acetone, and isopropanol in sequence, followed by drying at 80 ^oC in an oven overnight and then UV ozone treatment for 30 min. Then 25 μL of ZnO precursor solution was deposited on the ITO glass (4500 rpm for 40 s), then annealed at 200 °C for 20 min. Active layer solutions with polymer concentration of 10 mg mL^{-1} were prepared in chlorobenzene (CB) solvent with 3% 1-chloronaphthalene (CN) as additive. The active layer (D/A ratio 1:1.3) mixed with PTB7-Th, ITIC-Th and FBR-CN, was stirred overnight at the temperature of 70 °C. Then 25 μL of active layer solutions were spin-coated on the top of ZnO in a glove box full of nitrogen (N_2). After stirring, the films were annealed at room temperature in vacuum for 6 h. MoO_3(10 nm) and Ag (100 nm) were deposited as top electrodes, by thermal evaporation under 10^{-5} Pa. *J*-

V characterizations of all devices were performed under AM1.5G using a Newport solar simulator. EQEs were measured using a Newport EQE system.

Mobility measurements

Electron-only devices were fabricated with the architectures: ITO/ZnO/active layer/Al. Hole-only devices were fabricated using the architectures: ITO/PEDOT:PSS/active layer/MoO_3/Ag. Electron mobility and hole mobility data were calculated from J-V curves and fitting the results to SCLC method by using the equation:

$J = 9\mu\varepsilon_0\varepsilon_r V^2/8L^3$

Where μ is the electron mobility, ε_0 is the permittivity of free space, ε_r is the relative permittivity of the material, V is the voltage drop across the device and L is the thickness of the film.

Figures

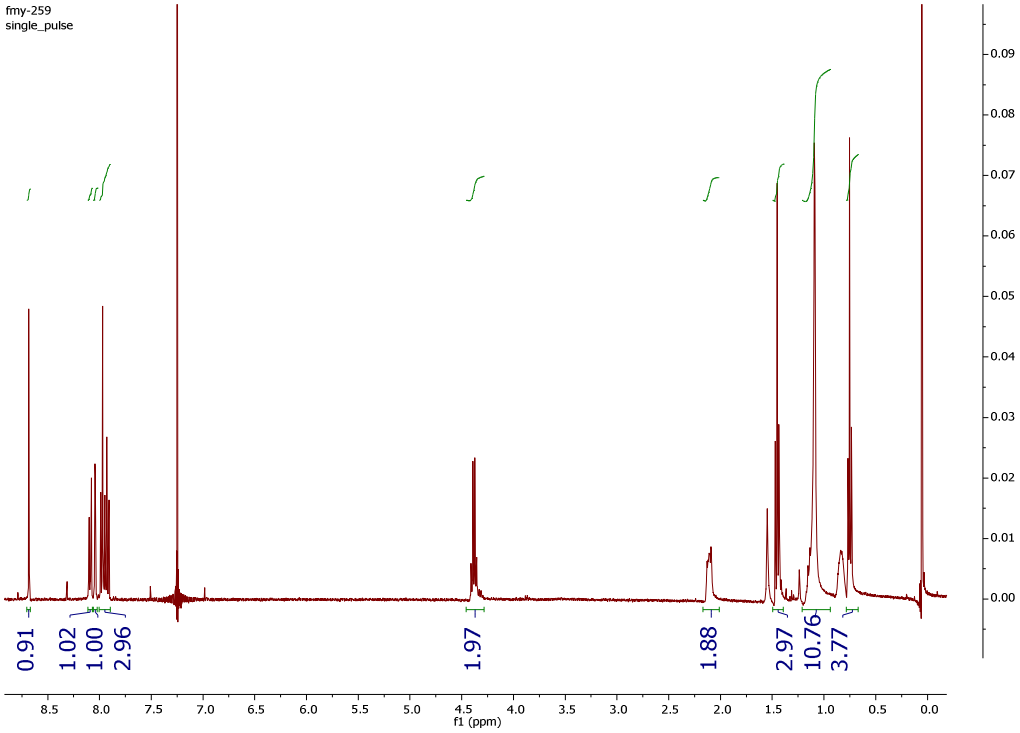

Figure S1. ^{1}H NMR spectrum of FBR-CN at 298K.

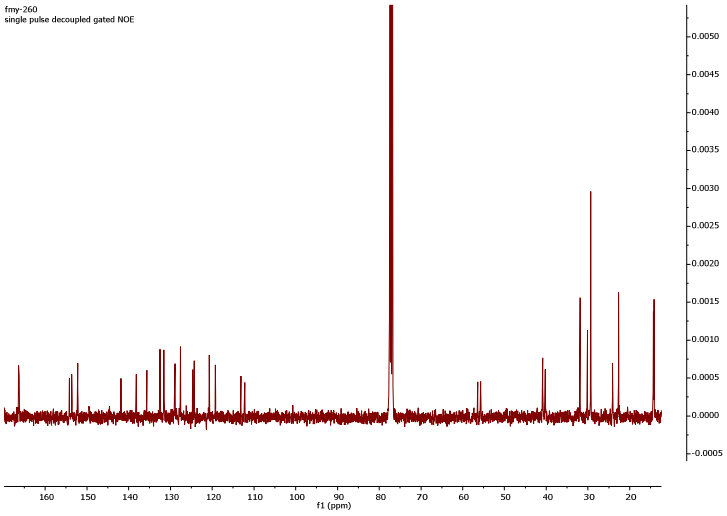

Figure S2. ^{13}C NMR spectrum of FBR-CN at 298K.

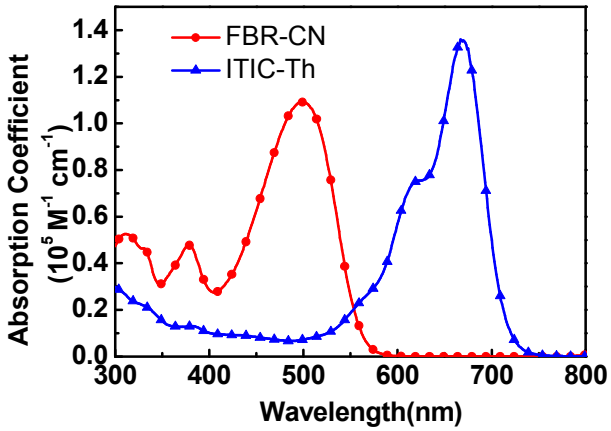

Figure S3. Absorption coefficient of FBR-CN and ITIC-Th in chloroform.

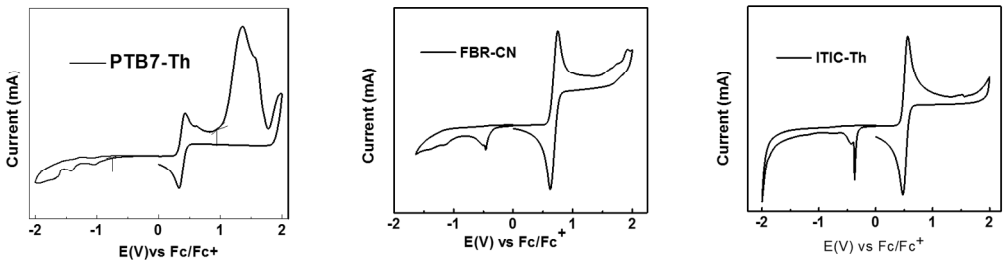

Figure S4. Cyclic voltammograms of PTB7-Th, FBR-CN and ITIC-Th in chloroform solution.

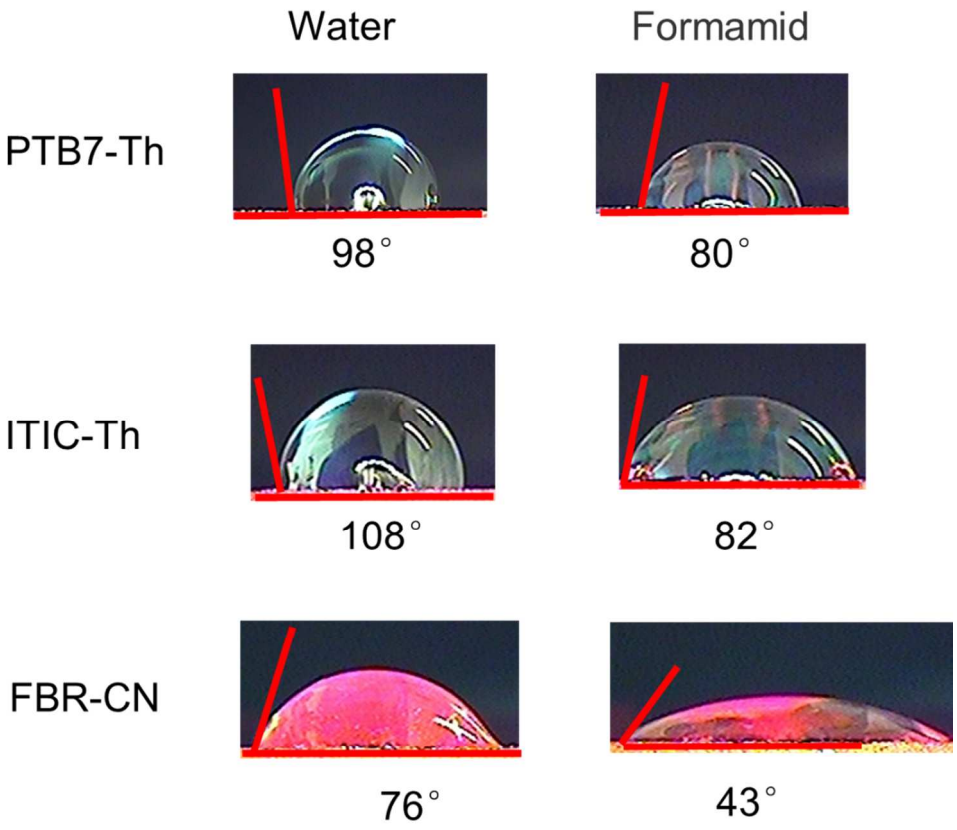

Figure S5. Contact angle of pure water and formamide on PTB7-Th, FBR-CN and ITIC-Th films.

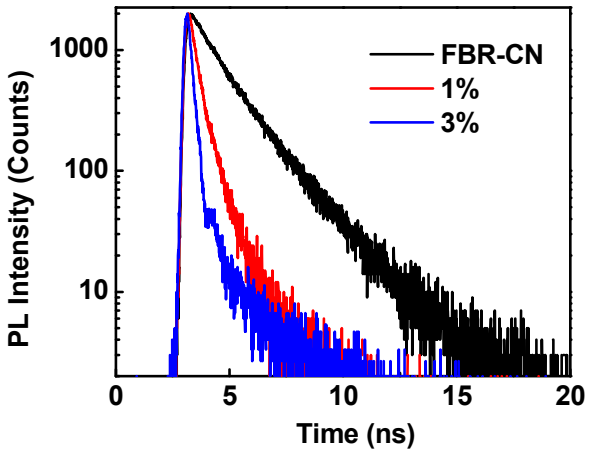

Figure S6. Time-resolved decay traces of pristine FBR-CN film, and FBR-CN blend with 1 or 3 wt% ITIC-Th.

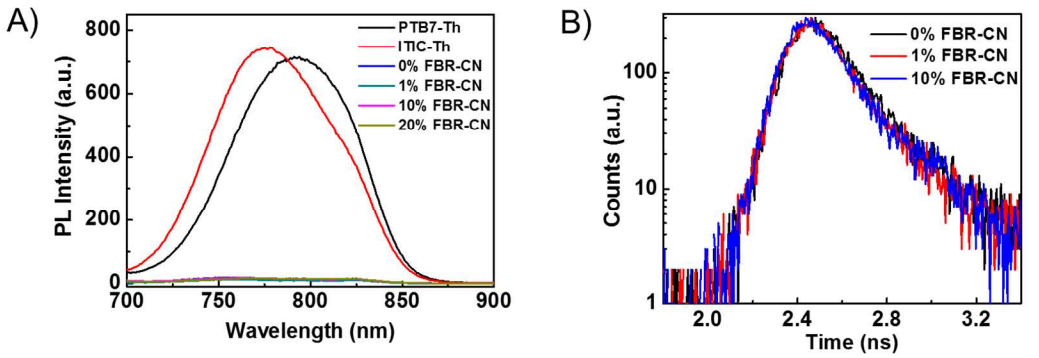

Figure S7. A) Steady PL spectra of PTB7-Th, ITIC-Th and PTB7-Th:ITIC-Th blends with varying content of FBR-CN. B) TRTPL spectra of PTB7-Th:ITIC-Th blends with varying content of FBR-CN.

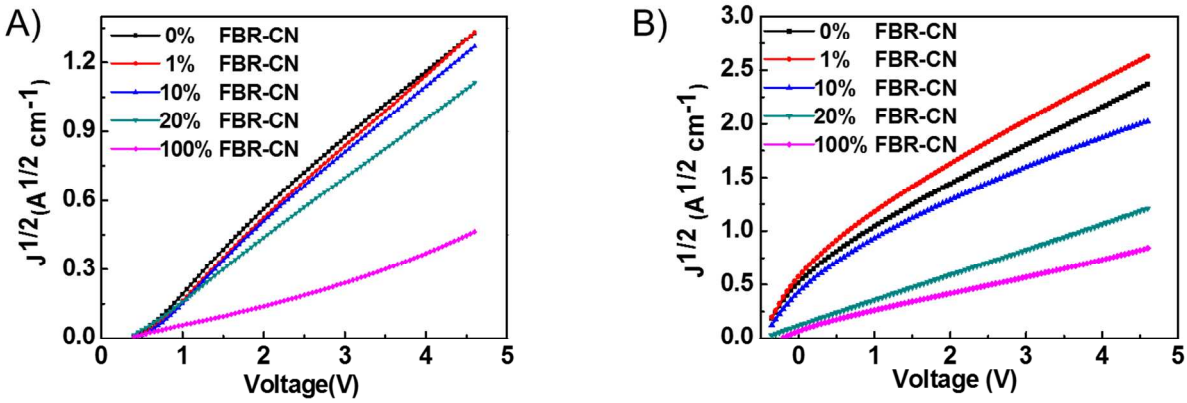

Figure S8. A) Electron mobility and hole mobility of PTB7-Th:ITIC-Th blends with varying content of FBR-CN.

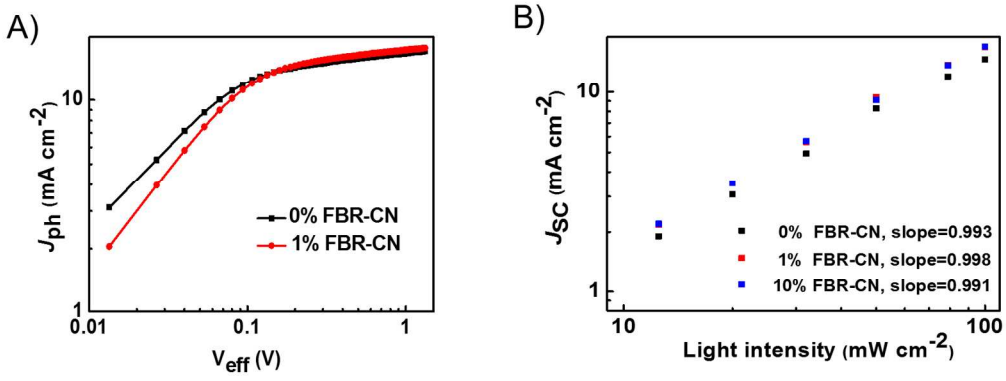

Figure S9. A) Photocurrent density (J_{ph}) versus effective voltage (V_{eff}) characteristics. B) Short current density (J_{sc}) versus light intensity of the ternary blends.

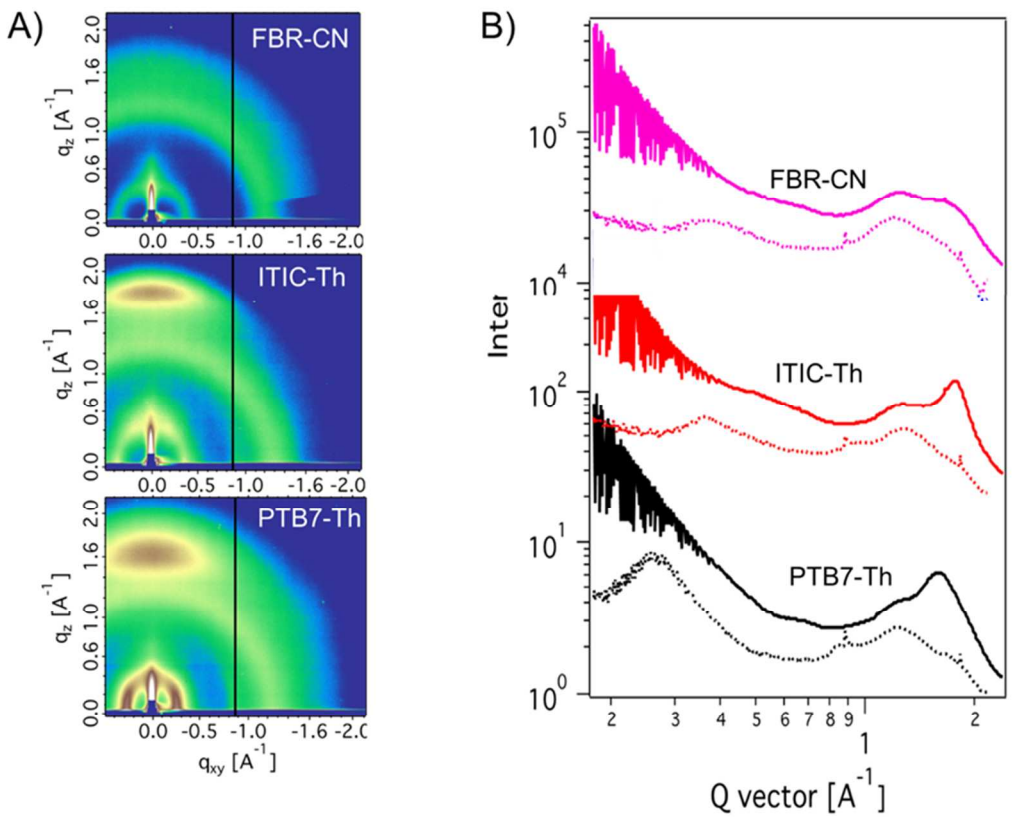

Figure S10. A) 2D GIXD images of PTB7-Th, ITIC-Th and FBR-CN neat film. B) The out-of-plane (solid line) and in-plane (dotted line) line-cut profiles of GIXD patterns of neat films.

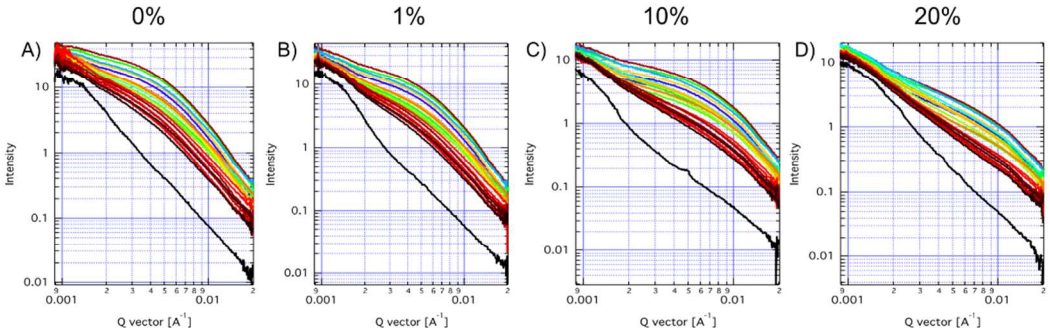

Figure S11. A, B, C, D) R-SoXS images of ternary OSCs with different FBR-CN contents.

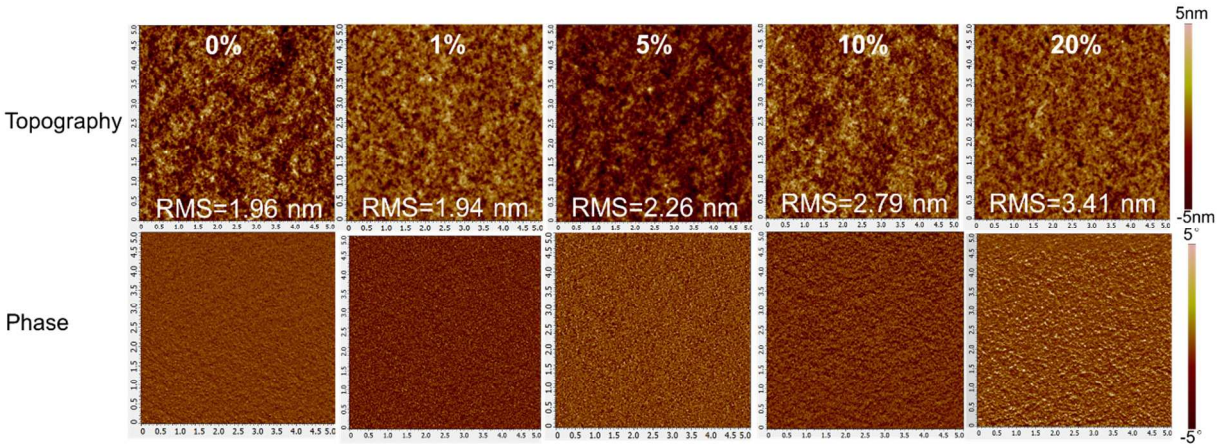

Figure S12. AFM images of PTB7-Th:ITIC-Th blends with varying content of FBR-CN.

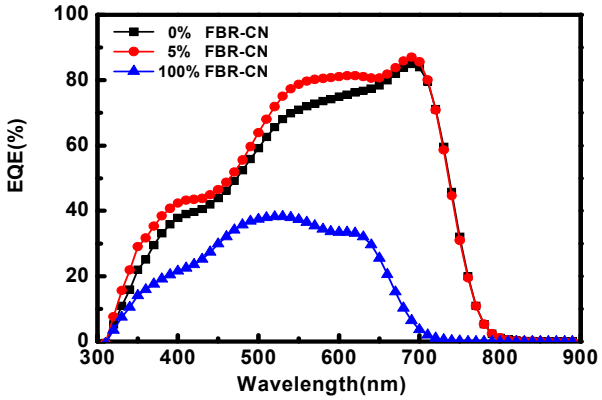

Figure S13. EQE curves of PBDB-T:ITIC-Th system with different FBR-CN weight ratios.

Table S1. Summary of photovoltaic parameters of ternary solar cells with different weight ratios of FBR-CN under AM1.5 illumination at 100 mW/cm^2.

FBR-CN (w/w)	V_{OC} (V)	J_{SC} (mA/cm^2)	FF (%)	PCE$_{ave}$ (max) (%)
0%	0.85±0.01	15.72±0.33	72.47±0.89	9.69 (9.88)
5%	0.86±0.01	16.65±0.07	72.43±0.56	10.37 (10.41)
100%	0.99±0.01	6.79±0.10	48.21±0.03	2.63 (2.71)